Solid Flow in the Annular Region of a Spouted Bed

The solid circulation in the annular region of a 0.146 and a 0.292 m ID semicylindrical and cylindrical air spouted beds was investigated for different spouting conditions. Stroboscopic photography, stopwatch and fiber optic methods were used to measure the vertical particle velocities in the annular region. The optical fiber probe enabled the measurement of particle velocities inside the dense annular phase and was validated at the walls. Velocity profiles in half beds were very different from those found in full beds. The work was then limited to full beds. Experimental results show that the solids flow is characterized by a point sink at the nozzle entrance with the solids moving almost in plug flow higher in the bed. There is negligible entrainment of solids along the spout wall and slow, thin wall layers are observed near the walls and spout. The velocity profiles are independent of the total height of the bed. A kinematic model successfully describes the observed velocity field.

Abdelhakim Benkrid
Hugo S. Caram
Department of Chemical Engineering
Lehigh University
Bethlehem, PA 18015

Introduction

Spouted beds are good gas-solid contactors for coarse particles ($dp > 500$ um) and provide good solid mixing and circulation. Detailed knowledge of the solids circulation pattern in a spouted bed is important to evaluate the effectiveness of gas-solid contact, the overall solids circulation rate and to understand the basis of operation of the device. Figure 1 illustrates the principal features of a steadily operating spouted bed. Spouting can be obtained by allowing a high velocity jet of fluid to enter a bed of diameter D_c and height H through a nozzle of diameter D_i. The high velocity jet forms a cylindrical cavity, the spout, that breaks through the bed surface and causes a stream of solids particles to rise rapidly. These particles, after rising above the peripheral bed level, rain back onto the annular region between the spout and the bed wall, where they slowly travel downward and radially inward towards the spout in the lower part of the annulus. Part of the gas flares out into the annular bed of solids surrounding the central core. Solid particles are circulated through the bed, resulting in efficient solid-fluid contact and a good solid mixing. The major part of the solids enter the spout in the lower part of the bed up to a height of approximately one bed radius. A dead zone is formed in the bottom region of flat bottomed spouted beds.

Early studies of fluid flow in a spouted bed were made by Mamuro and Hattori (1968) and Lefroy and Davidson (1969). They proposed a semi-empirical pressure distribution in the spout and found the pressure and fluid flow distributions in the annular region. At maximum spoutable height the pressure gradient at the top of the bed was enough to fluidize the bed material at the top. Lefroy and Davidson (1969) also solved the continuity and momentum equations in the spout to find the rate of solids entrainment. No details of the solid flow in the annular region were provided.

This work was generalized to beds below the maximum spoutable height by Grbavcic et al. (1976), Littman and Morgan (1980), and Epstein and Levine (1978). These authors accounted for the turbulent motion of the fluid in the annular region and found that the local gas flow and pressure gradient in the annulus was independent of the total bed height.

The study of the solids flow in the annulus followed two routes. Experimental flow observations were carried out at the flat face of semi-cylindrical spouted beds by Thorley et al. (1955, 1959), Lim and Mathur (1974), and Suciu and Patrascu (1978). They observed more or less uniform solid entrainment along the spout wall. This matched the observed linear decrease of the particle vertical velocity along the walls of cylindrical spouted beds. Unfortunately, Rovero et al. (1985) and Benkrid et al. (1984) showed that semicylindrical (half) spouted beds were a poor representation of the solids flow in cylindrical (full) beds.

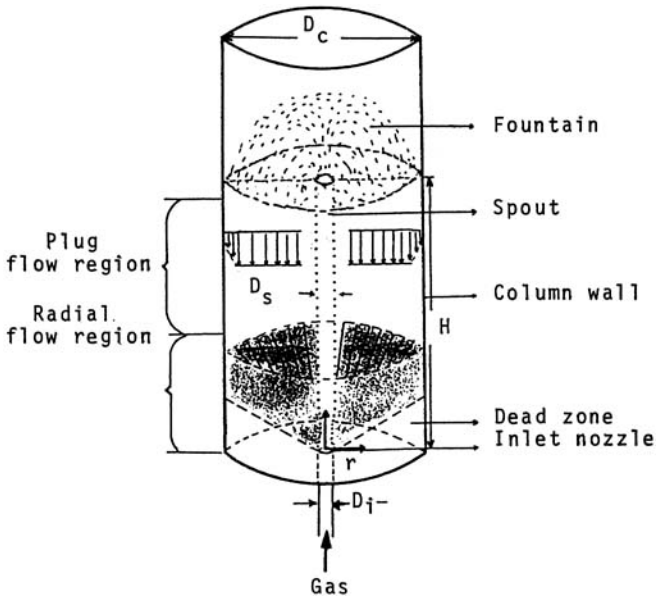

Figure 1. A spouted bed.

The Mechanics of Solid Motion: Plastic and Kinematic Models

The mechanics of solids in the annular region was studied in reference to the spout wall stability by Bridgwater and Mathur (1972), McNab and Bridgwater (1974), and Khoe (1980) by using the theory of plasticity. They did not extend the work to the prediction of the velocity field. The plastic theory, being really a theory of statics extended to the case of creeping flow, supplies only the stress distribution in the static material and not the velocity field. Further assumptions must be added to determine the velocity distribution [Jenike (1954), Spencer (1964) and, more recently, the review by Jackson (1986)]. Although the principles of the method have been discussed in detail little progress has been made in the prediction of velocities in specific cases. Coaxiality of the principal axes of deformation and stress is the standard assumption in most cases and has been used to try to predict the flow field in two dimensional spouted beds by Amirshahidi (1984) and in axisymmetric beds by Sullivan, Benkrid and Caram (1987). Unfortunately for the simplified stress fields proposed, and due to the hyperbolic nature of the equation, the solutions are oscillatory. Since no oscillations have been observed experimentally, the theory is suspect, and models that predict a smooth velocity field are probably more suitable for this study.

Kinematic theory

Nedderman and Tuzun (1979) and Graham et al. (1987) used a kinematic model based on the work by Litwiniszyn (1956, 1963) and Mullins (1974) to describe the flow of granular material in discharging hoppers. The following description is based on the references given above.

The model assumes that particles move downward to fill the empty spaces left by particles removed from below. No mechanism is postulated to determine how fast the particles will be removed or the cause of the removal of the first layer. This information must be provided as an input to the model. The key assumption is that the horizontal velocity is proportional to the gradient of vertical velocities and is given by:

$$u = -B\frac{\partial v}{\partial r} \tag{1}$$

where the constant B depends on the material and must be determined experimentally. Since it has dimensions of length it is expected based on dimensional analysis to be proportional to the particle size. The equation is then combined with the continuity equation in cylindrical coordinates

$$\frac{1}{r}\frac{\partial(ru)}{\partial r} + \frac{\partial v}{\partial z} = 0 \tag{2}$$

to give an equation for the vertical velocity

$$\frac{1}{r}\frac{\partial}{\partial r}\left(r\frac{\partial v}{\partial r}\right) = \frac{1}{B}\frac{\partial v}{\partial z} \tag{3}$$

This is a parabolic equation that can be solved specifying as boundary conditions the rate of entrainment into the spout and no flow across the bed walls. It is important to notice that the solution propagates from the bottom up and is independent of the total height of the bed. Since, as will be discussed below, the observed flow patterns were independent of the total height of the bed and it is reasonably easy to obtain solutions to Eq. 3, the model will be used extensively.

Solids velocity measurement in spouted beds

Most work has been limited to the measurement of the velocity at the external walls. This is done in the slow moving dense phase ($v \sim .01$ m/s) by timing individual particles for a fixed distance or using strobe photography. In the faster moving regions and in the spout, high speed photography has been used by Thorley et al. (1959), Lefroy and Davidson (1969), Suciu and Patrascu (1978), and others. Solid velocities in the interior of the bed were measured by Rovero et al. (1985) using a bed initially seeded with tracer layers. The gas flow was periodically stopped to find the location of the tracers as a function of time. Radioactive pills were used by Van Velzen et al. (1974) to follow the position of a single particle in the bed.

A fiber optics probe, originally proposed by Oki et al. (1977) for use in fluidized beds and further developed by Patrose and Caram (1982), was used in this work. A schematic of this probe is shown in Figure 2. The technique measures the time delay between the light signals received by two optical fibers separated by a small effective distance 1. For a delay τ the velocity is given by

$$v = \frac{L}{\tau_m} \tag{4}$$

The time delay is computed from the delay that makes the cross correlation between the signals received, $C(\tau)$, by the two fibers

$$C(\tau) = \lim_{T\to\infty}\frac{1}{T-\tau}\int_{\tau}^{T} A(t)B(t-\tau)\,d\tau \tag{5}$$

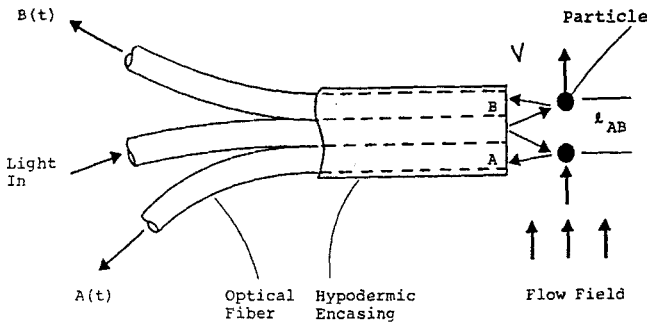

Figure 2. The optical fiber probe in a flow field (after Patrose and Caram, 1982).

Light emitted by the illuminating fibers and reflected by the moving media is collected by fibers *A* and *B*. The delay between the signals collected by *A* and *B* is used together with the effective distance between fibers to compute the velocity.

a maximum. Further details are given by Patrose and Caram (1982).

Experimental. Two different plastic columns with a flat base and internal diameters of 0.146 and 0.292 m were employed. The large column had a variable inlet nozzle diameter while the small column had an inlet nozzle diameter of 0.0127 m. Half sectional columns with the same geometry of the full vessels were used. Their flat wall was made of plate glass to facilitate the observation of the spout and the particle motion. Humidified air, to reduce static effects, was used as spouting fluid and its flow was measured using a rotameter bank. Glass beads of three different sizes (Potters Industries, New Jersey; P-047, $d_P = 0.95$ mm, A-170, $d_P = 1.68$ mm, A-205, $d_P = 2.05$ mm) and wheat (average dimensions 2.7 × 5.7 mm) were used as a bed material.

Probe construction and validation

A 0.15 m long by 1.6 mm outside diameter fiber optic probe was constructed of stainless steel tubing for mechanical strength and rigidity. The fibers had silica cores with a core diameter of 150 μm surrounding by plastic cladding. Five illuminating fibers and two receiving ones were used with illumination provided by a halogen lamp. The individual fibers were 0.125 mm in diameter and the outer diameter of probe tip was 1.6 mm. To ensure good light transmission through the probe, the ends of the fibers at the tip of the probe were wet polished with fine emery paper, and then finished on a felt polishing wheel with an aqueous suspension of 0.0001 mm aluminum powder.

The light signals were detected by PIN photodiodes. The resulting electrical signal was filtered for high frequencies and fed to a Honeywell Saicor 43A correlation and probability analyzer. The cross-correlation function generated by the analyzer was displayed on a digital oscilloscope and the transit time was read as the maximum of the cross-correlation curve. A discretization error of 2–5% percent was expected in the reading of the time delay. The effective distance between the two receiving fibers, slightly different from the geometrical distance, was obtained by calibrating the probe on a rotating disk of known angular velocity ω. The slope of the plot of the tangential velocity ωr as a function of the inverse of the time delay $1/\tau_m$, shown in Figure 3a, gives an effective distance of 0.324 mm.

Three different experiments were used to test the probe readings in air spouted beds. In the first experiment, particle velocities were measured with the probe at the transparent wall surface and then compared to stopwatch readings. These measurements were performed using ink stained glass beads tracers traversing a 20 mm band. Secondly, the effect of the invasiveness of the probe on the flow was studied by inserting the probe across the radius and at a shallow angle across the semicylindrical bed near the flat wall. Figures 3b and 3c show that there is good agreement between the stopwatch and the probe measurements in both cases. A third experiment consisted of obtaining velocity data using two different probes to determine the effect of the probe diameter on the measured particle velocities. Good agreement was found between the results obtained with 1.6 and 0.9 mm probes.

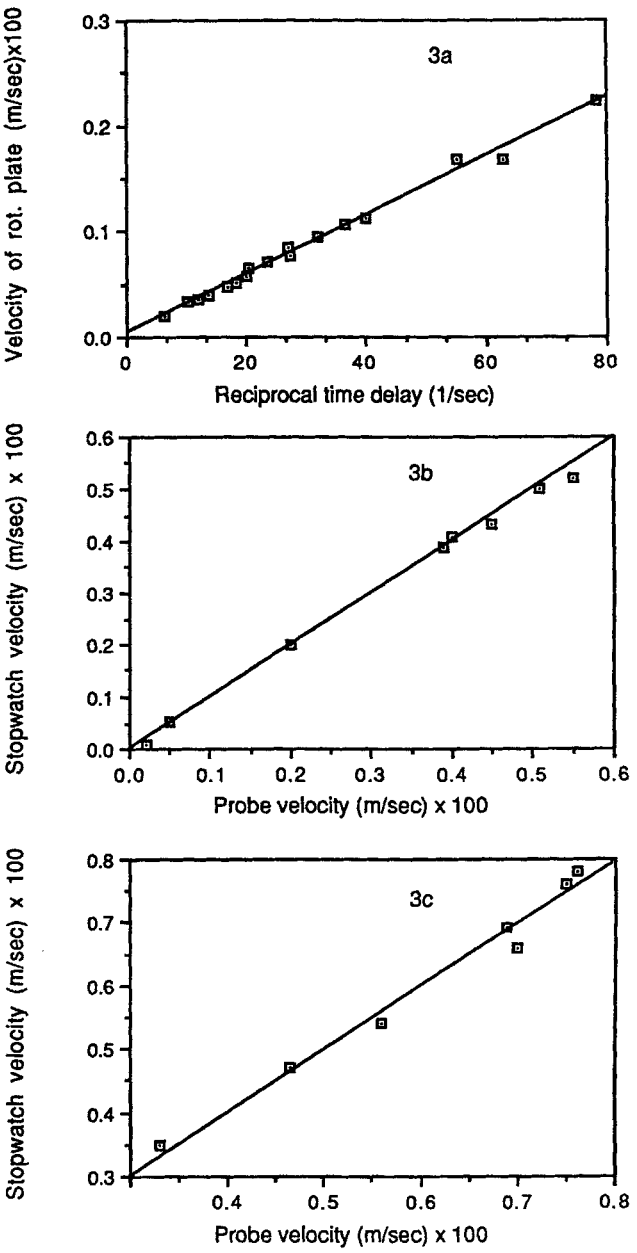

a. Calibration curve
b. Stopwatch wall data vs. probe measurement
c. Stopwatch wall vs. probe measurement (probe approaching the wall from the inside)

Figure 3. Probe calibration and validation.

Table 1. Operating Conditions

Run	Type	Height $m \times 10^2$	Gas Flow $m^3/s \times 10^6$	Column and Nozzle Dia. $m \times 10^2$
1	P-047	24.00	8022	15.24-1.27
2	Wheat	40.64	8730	15.24-1.27
3	A-170	40.64	12269	15.24-1.27
3*	A-170	34.29	11797	15.24-1.27
4	A-170	25.40	11797	15.24-1.27
5	A-205	27.94	12741	15.24-1.27
6	A-170	36.83	28786	29.21-5.08
7	A-170	34.29	10854	15.24-1.27
8	A-170	36.83	27606	29.21-5.08
9	A-170	19.05	variable	15.24-1.27
10*	P047	24	6107	15.24-1.27

Run 10* is performed on a half-bed configuration.

For the actual measurements, holes were drilled at approximately every 25 mm along the z-axis of the half and the full beds. The sampling procedure consisted of introducing the fiber optic probe radially to the desired r and z position where three or more readings of the transit time were taken and the average transit time determined. Operating conditions for each of the runs are given in Table 1.

Results and Discussion

Velocity measurements in half vs. full beds

Measurements of the downward solids velocity were carried out in full and half beds at fixed superficial air velocities, four different bed levels (75, 125, 175, 225 mm from the bottom) and five or more radial positions in both full and half beds. The left side of Figure 4 compares the measured vertical velocities at two perpendicular planes in a full bed. The full bed appears to be essentially symmetric so that measurements for the cylindrical bed can now be reduced to a single radial plane. The half bed measurements were carried out at the flat wall and at radial planes $\pi/4$ and $\pi/2$ rad to the flat wall. The results displayed in the right side of Figure 4 indicate that the vertical velocity in the annulus depends on both the angular and radial position of the probe with respect to the flat wall. This figure also shows that the velocity increases in the angular direction away from the flat wall and the lowest velocities are observed at the flat wall itself. The velocities at the radial plane normal to the wall approximate the values of the plug flow profile observed in the full bed as is shown in the left side of Figure 4. The agreement is fair at the top of the bed but the quantitative similarity disappears as we approach the bottom region. Similar observations were made by Rovero et al. (1985). Consequently, velocity profiles based on measurement on the flat wall of a semi-cylindrical spouted bed are poor representations of the conditions in a full bed. This casts some doubt on previous work, like that of Lim and Mathur (1978), based on the flat wall data. We find that velocities are much smaller and qualitatively different than those measured in the full bed. This also explains why efforts by Green and Bridgwater (1983) to model full bed behavior using wedge shaped beds have not succeeded, although some authors have measured similar wall velocities in full and half beds of wheat and millet (Geldart and Whiting, 1980; Geldart et al., 1981). In light of these results, the work will focus in full beds only.

Vertical velocities in full beds. Some of the detailed measurements for the 0.146 m and 0.292 m, are shown in Figures 5 and 6. Figure 5a indicates that in the upper part of the annulus and approximately one bed radius above the base of the bed, the solids moved almost in plug flow. Near the walls and at the spout-annulus interface, a relatively thin wall layer of about 5 particle diameters thick was observed as can be seen in Figures 5a and 6a. Since the vertical solids velocities did not change with distance from the bottom, this indicated that, within the experimental error, little or no entrainment of solids into the upper part of the spout region occurred, although there was some recirculation at the very top of the bed. In the bottom region, however, figs. 5b and 6b show that the solids velocity increased as the particles approached the bottom of the bed and the spout-

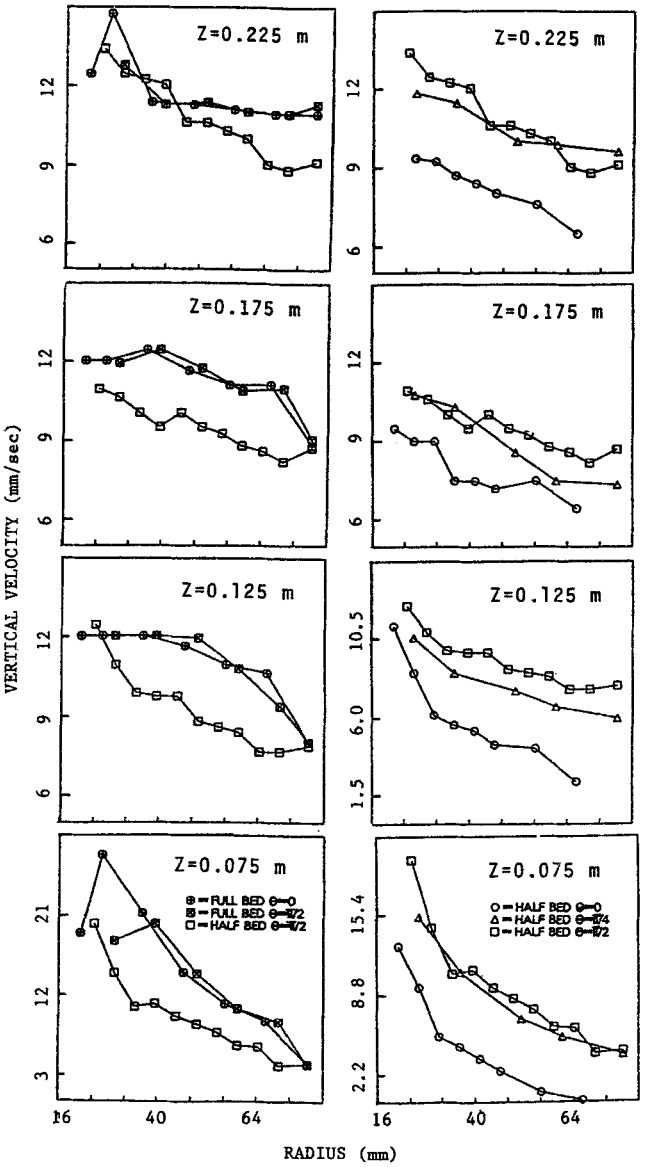

Figure 4. Vertical velocities in full beds (F.B.) vs. half beds (H.B.) at different heights and angles (l) for constant superficial gas velocity (run 10).

Measurements in full beds were done at two perpendicular radial planes (l = 0, /2), while in the half bed were done at the wall and at radial planes at /4 and /2. Full bed appears symmetric, while half bed show much lower velocities especially at the wall.

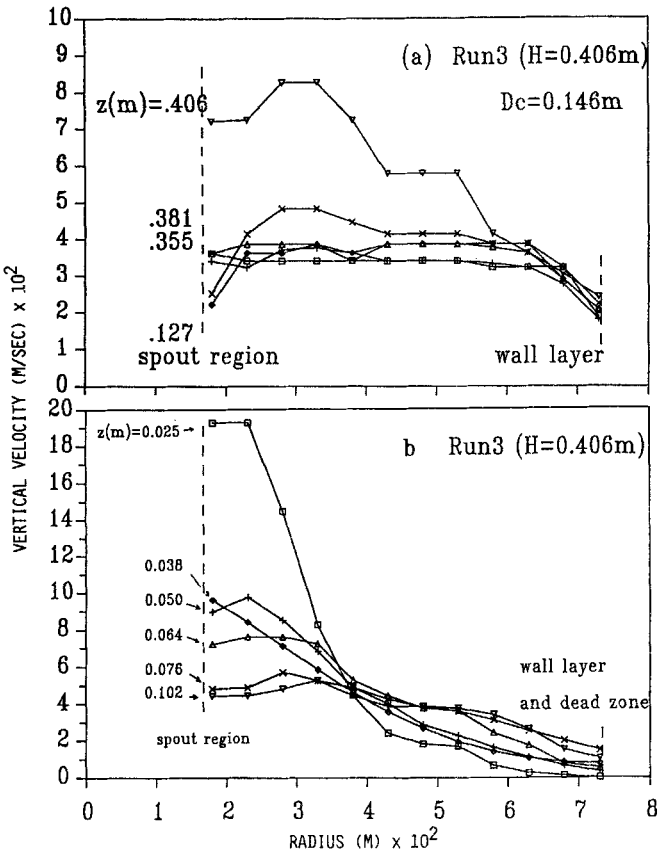

a. $0.127 < z < 0.406$ m
b. $0.0254 < z < 0.1016$ m.

Figure 5. Vertical velocities in the 0.146 m full bed for run 3 at different heights in the bed.

Velocity profiles for heights between 0.127 and 0.355 m cannot be differentiated except at the wall where a thin wall layer is formed. The particles also slow down near the spout wall. Detailed wall data are in Figure 8.

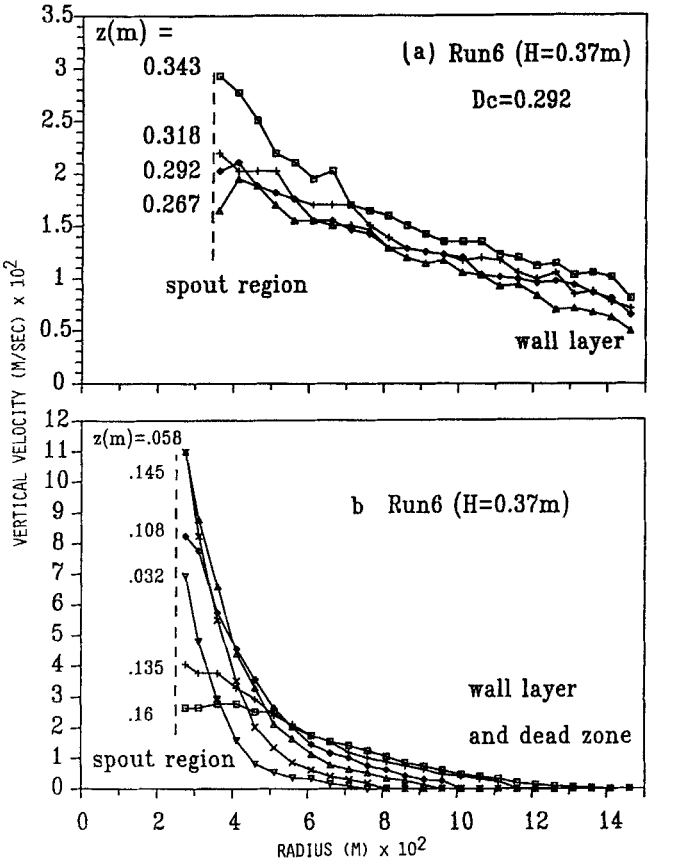

Figure 6. Same as Figure 5 but for the 0.292 m full bed (run 6).

The profiles are qualitatively similar to those found near the bottom of the smaller bed. The bed is not tall enough to show a plug flow region.

annulus interface. These velocities were much higher than those observed in the upper part of the bed.

Overall solids circulation and wall velocity

Particle velocity measurements as those shown in Figures 5 and 6 were used to compute the solid circulation as a function of height in the bed. An example of these computations of the volumetric solid flow rate as a function of height is shown in Figure 7 and was obtained using Simpson's rule to numerically integrate the particle velocity profiles over the entire cross sectional area of the annulus at each level. The data shown in Figure 7 correspond to runs 3 and 3*. Both runs were carried out in the 0.146 m bed with essentially the same gas flow rate but with different total bed heights. Disregarding the top of the annulus, it is striking that the rate of solids circulation is almost independent of the bed height for beds shallower than the maximum spoutable height and that the solid circulation rate does not change with position in the bed. In this figure we also notice that the calculated solids flow rate in run 3 is much higher at the top of the bed than in run 3*. This is due to the fact that in run 3 the bed is at its maximum spoutable height and the top of the annulus has become fluidized with the corresponding higher velocities.

As done by Thorley et al. (1955, 1959), most investigators have computed the solid circulation from measurements in the

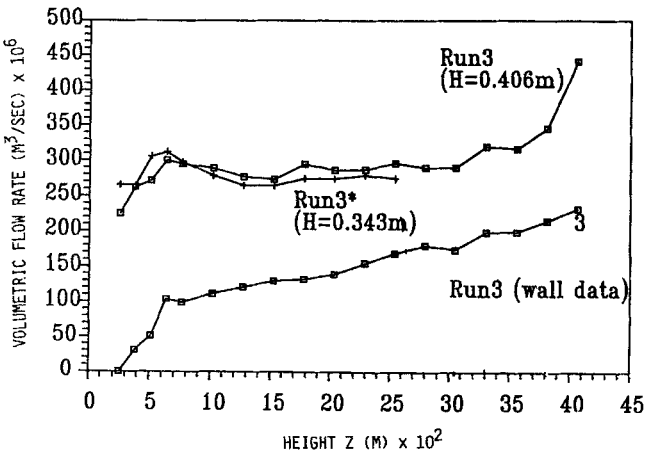

Figure 7. Volumetric solids flow rate in the annulus as a function of height in the bed for two different total bed heights and similar gas flow rates (Runs 3 and 3*).

Solids flow rates are obtained by integrating the probe data. Solid entrainment into the spout is limited to the bottom region. Also shown are the flow rates computed assuming the solids move in plug flow at the wall velocity. They seriously underestimate the total flow.

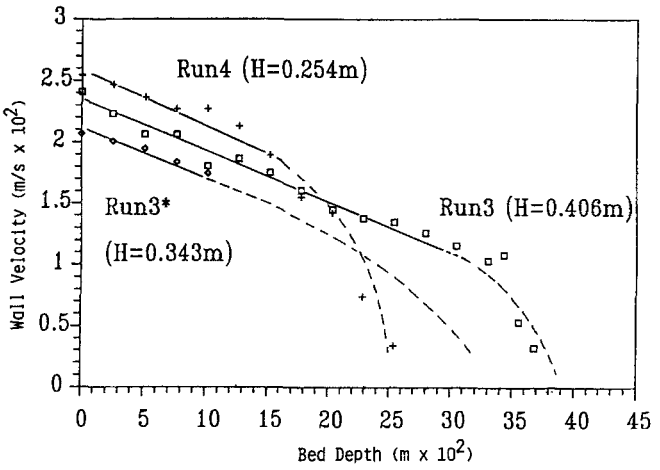

Figure 8. Solids velocity at the wall in the 0.146 m bed for three different total bed heights and almost identical gas flow rates (runs 3, 3*, 4).

It was plotted as a function of distance from the top of the bed, the wall velocities almost overlap.

external wall. Figure 7 provides a comparison of the results of this work with the values that would be obtained if the values of the velocity at the wall had been used to compute the volumetric solid flow rate in the annulus. As found by Thorley (1955, 1959) the volumetric flow rate appears to decrease linearly with height in the bed, but it is very different from the volumetric flow rate computed by integration of our data. The difference is caused by the presence of the thin slow layer near the wall, that hides the true velocity profile.

Figure 8 shows the wall velocities for different total bed heights, same gas flow rates (runs 3, 3* and 4), plotted as a function of depth, or distance from the top of the bed. The plots almost overlap but this also indicates that if one were to compute the volumetric flow rate from the wall velocities, the volumetric flow rate would depend on the total bed height. This is opposite to the experimental observations presented before. Finally, the overlapping of the plots appears to indicate that the effect of the wall propagates from the top down as it would do in a boundary layer.

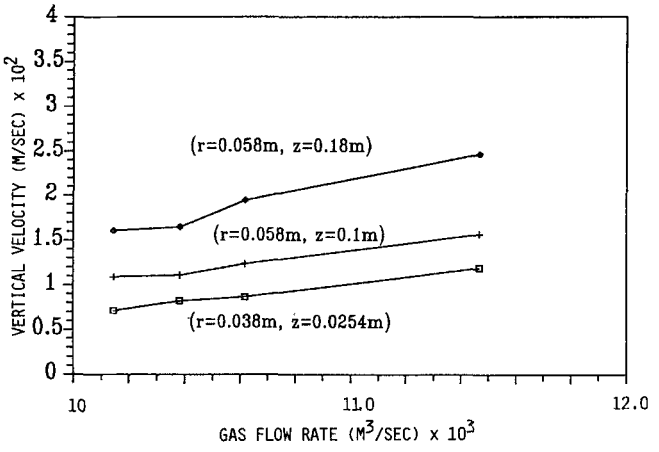

Figure 9. Particle velocities in the 0.146 m full bed as a function of the gas flow rate at three different locations.

Effect of the gas flow rate on the solids circulation

The effect of the gas flow rate on the solid circulation was also investigated. Figure 9 shows that for a given bed depth increasing the spouting gas rate increased the downward particle velocity in the annulus, and correspondingly, the solid circulation rate. Thorley et al. (1955, 1959) calculated the solids circulation rate in the annulus by using the particle velocities measured at the wall of a semicylindrical spouted bed of wheat. They also found that the circulation rate of solids increases with the gas flow rate. Note the relative narrow range of gas flow rates where the bed can operate. There is a minimum spouting velocity and at high flow rates the top of the bed becomes fluidized. The range of permissible gas flow for stable spouting becomes narrow as the total bed height approaches the maximum spoutable height for a given material and column geometry. A similar observation can be found in Mathur and Epstein (1974) and is a significant feature of the operation of spouted beds.

Radial flow

The vertical velocity data show (Figures 5a and 6a) that in the bottom region of the annulus the particle velocities increased dramatically. This velocity profile suggests a point sink and radial flow of solids in this region. In the neighborhood of the point sink the velocity will be directed in the radial direction, as proposed by Brown and Richards (1970) for the flow in discharging hoppers. For an axisymmetric incompressible radial flow the volumetric flow of solids per unit solid angle

$$\Lambda(\theta) = v_r R^2 \tag{6}$$

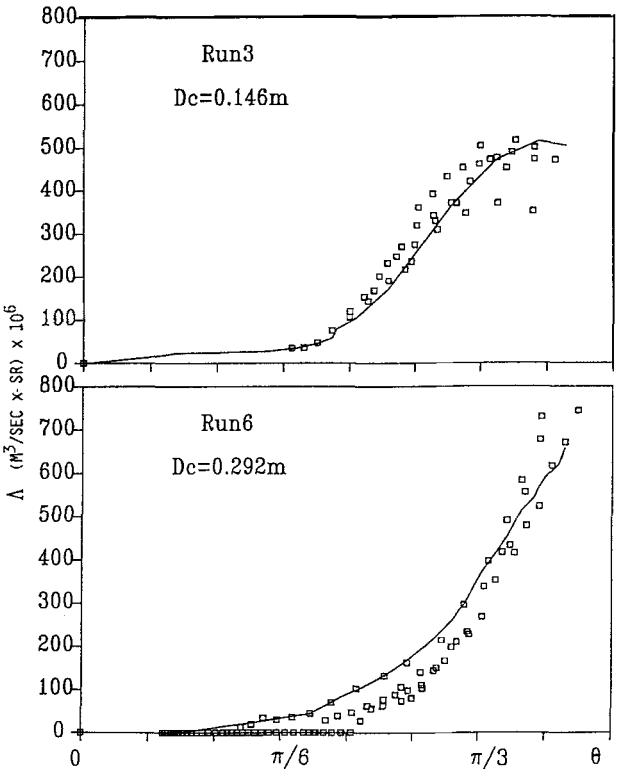

Figure 10. Volumetric solids flow rate per unit solid angle as a function of the angle between the horizontal and the radial direction considered.

should be a function only of the angle θ between the horizontal and the radial direction considered. If the radial flow hypothesis were to hold, experimentally determined values of $\Lambda(\theta)$ should collapse into a single curve if plotted as a function of the angle θ. Since only the value of the vertical component is measured the value of Λ must be computed as

$$\Lambda(\theta) = \frac{v(r^2 + z^2)^{3/2}}{z} \tag{7}$$

Figure 10 shows that the hypothesis is satisfied locating the point sink 7.5 mm below the gas inlet for measurements in the 0.146, and 0.292 m beds. The scattering observed at high angles may be due to the proximity of the spout wall.

A kinematic model of the flow

As discussed above the vertical velocity can be modeled using Eq. 3. The boundary conditions for this equation must reflect no flow across the wall and the bottom. The spout itself is seen by the bed as a line sink. The line sink is specified by the flow of solid converging to it per unit height and radian as a function of height. The resulting conditions are:

$$\begin{aligned} &\text{at } z = 0;\ v = 0 \\ &\text{at } r = R_w;\ u = 0 \\ &\lim_{r \to 0} r\,u = f(z) = \delta(z)\pi R_w^2 v_o \end{aligned} \tag{8}$$

The value of $f(z)$ proposed describes a point sink at the bottom, as expected from the experimental observations. This is an initial-value problem and the solution propagates from the bottom up. This coincides with the observations of Grbavcic et al. (1976) which indicate that the fluid flow and pressure gradients are independent of the total height of the bed. Moreover, the experimental observations presented here indicate that the solid flow patterns are also independent of the total bed height. Standard methods (Carslaw and Jaeger, 1959) give the series solution:

$$v(r, z) = v_o \sum_{n=0}^{\infty} \frac{J_o(\lambda_n r/R_w)}{J_o^2(\lambda_n)} \exp\left(-\lambda_n^2 Bz/R_w^2\right) \tag{9}$$

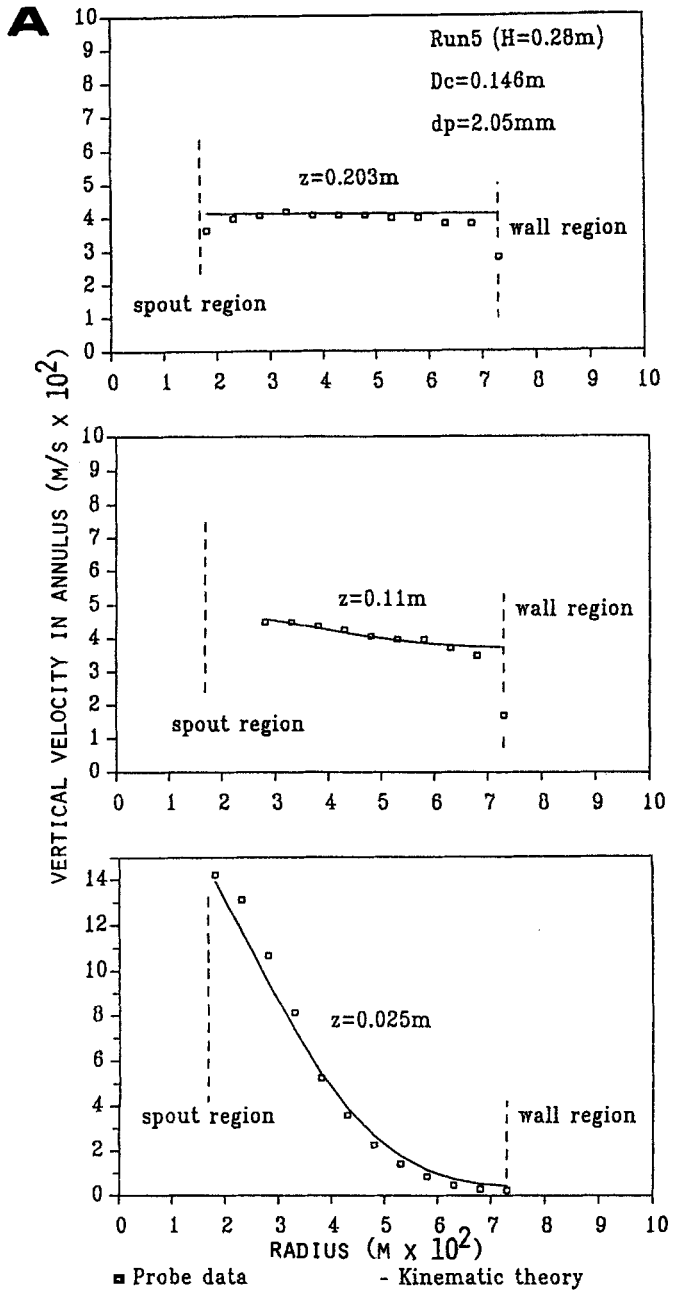

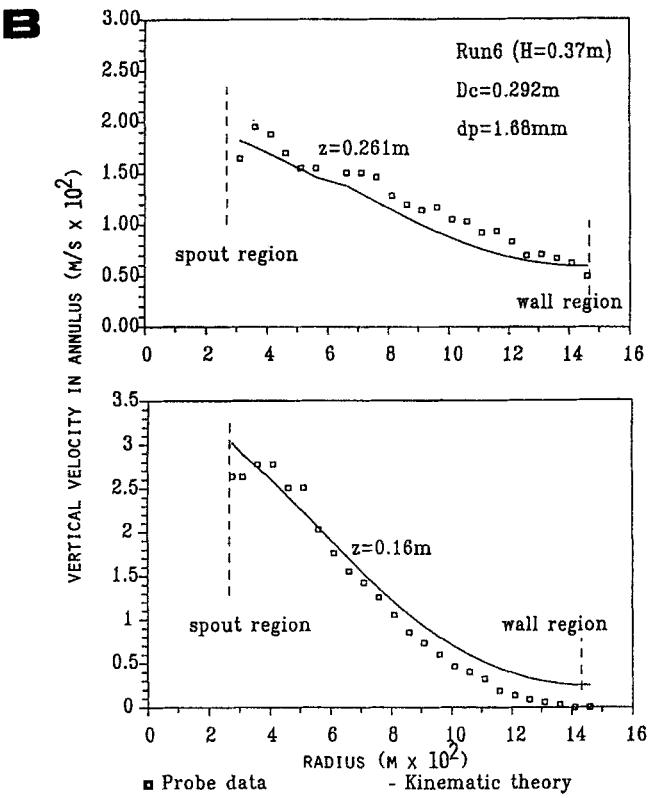

Figure 11. Representative comparison of the predicted and measured velocities for different bed and particle sizes: a. run 5; b. run 6.

Where v_o is the superficial particle velocity in the annulus, λ_n are the zeroes of J_1, the Bessel function of order one, and J_o is the Bessel function of order zero. This equation depends on two experimental constants, v_o and B. For the model to be useful, the parameter B should be independent of the bed size and by dimensional analysis, proportional to the characteristic particle dimension, i.e., $B = kd_p$; the proposed correlation should be applied to at least two particle sizes. Using a trial and error method, a value of the kinematic constant B that fits the velocity distribution data for run 3 was found to be equal to five times the maximum sieve size for the particle mixture. Figures 11a and 11b show the good agreement between the model and the experimental data for the 0.292 and 0.146 m beds and particles mixtures of average diameters of 1.68 and 2.05 mm with maximum sieve sizes of 2.36 and 2.0 mm, respectively. Graham (1987) reported values of k obtained for the discharge of hoppers to be between 0.5 and 9.0 particle diameters. It should be stressed that spouted beds and discharging hoppers are different systems where the mechanisms of solid motion are different, so these values should only be used as a reference. Note that in Eq. 9 a dimensionless velocity $v^* = v/v_0$ will be only a function of the dimensionless radius $r^* = r/R_w$ and height $z^* = Bz/R_w^2$. Using the dimensionless variables, one obtains a "universal" velocity profile in the annulus valid for any cylindrical spouted bed. Any two spouted beds having the same dimensionless height will have geometrically similar solid flow patterns. This "universal" solid flow pattern is shown in Figure 12. Since the vertical distance scales with the square of the radius, larger diameter beds appear shallow from the point of view of the solid circulation. Finally, a plot of the volumetric radial flow Λ, based on the vertical velocity equation fits well the experimental lines shown in Figure 9.

Summary and Conclusions

Carefully validated fiber optics velocity measurements in the annular region of the spouted bed offered a view of the solid flow that was quantitatively and qualitatively different from that established in the literature at the time of this writing. To extend the basis of comparison and since half beds have been widely used to study solid motion in spouted beds, velocity profiles in half and full beds were compared. Velocities were much higher in full beds and qualitatively different from those in half beds. This partially invalidated previous data taken in half beds and narrowed the investigation to full cylindrical beds. Vertical velocity measurements in full beds showed the following regions: A *plug flow zone* in the upper part of the annulus where the particles moved at uniform velocity. Some disturbance was observed at the top where the flow is perturbed by the fountain. Solids leaving the plug region entered the *radial flow region* where they converged to an apparent point sink located slightly below the base of the bed. Close to the external wall and the spout boundaries a *thin wall layer* (about five particle diameters) provided a sharp transition between the bulk velocity and the much slower wall velocity. Finally, a *dead zone* was formed at the bottom of a flat bottomed bed. The velocity profiles were unaffected by the total height of the bed.

The overall solid circulation was found to remain constant along the length of the bed indicating that except at the bottom region there is no entrainment across the wall of the spout. This is in contrast with earlier studies predicting uniform entrainment along the length of the spout. Circulation rates were also compared with predictions based on velocities at the wall. Since the latter were much smaller than the bulk velocities they underpredicted the overall circulation rate.

The effect of the gas flow on the solids velocity was studied in the 0.146 cm bed. Particle velocities increased with the gas flow rate in the narrow range between minimum spouting and spouting instability when the top of the bed becomes fluidized. That range becomes narrower as the total bed height approaches the maximum spoutable height.

The particle flow was modeled using a purely kinematic model (Nedderman and Tuzun, 1979). The model depends on two experimental parameters, the total rate of solids circulation, and the kinematic constant B. For a value of B equal to five times the maximum sieve size for the particle mixture and experimentally determined overall circulation rates, the model predicted well the velocity profiles and particle trajectories. The non trivial dimensionless variables yielded a universal particle dimensionless velocity profile for the annular region. This provided a scale-up criterion for the solid circulation.

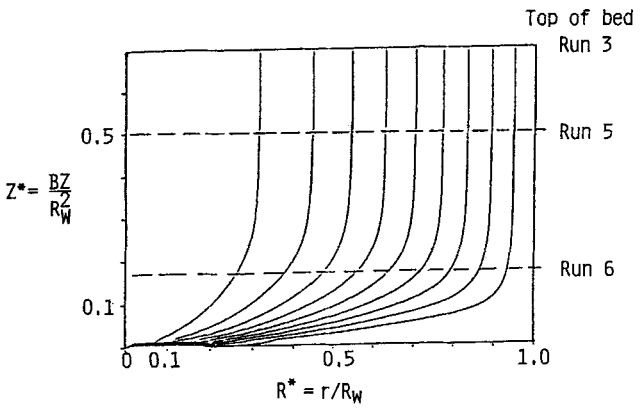

Figure 12. "Universal" streamlines as predicted by the kinematic model.
The dashed lines represent the dimensionless heights of the beds for runs 3, 5 and 6.

Notation

$A(t)$, $B(t)$ = light signals collected by the receiving fibers
$C(\tau)$ = Cross-correlation between light signals a and b
B = kinematic model constant, m
J_o = Bessel function of order zero
L_{ab} = effective fiber separation, m
r = radial distance in cylindrical coordinates, m
r^* = dimensionless radial distance in cylindrical coordinates
R = radial distance in polar coordinates, m
R_w = bed radius, m
u = radial velocity, m/s
v = vertical velocity, m/s
v_r = radial velocity directed to the pole, m/s
v_o = superficial solid velocity in the annulus, m/s
v^* = vertical velocity
z = vertical coordinate, distance to bottom, m
z^* = dimensionless vertical coordinate

Greek letters

Λ = volumetric flow rate per unit solid angle, m^3/s
τ = time delay, s
τ_m = time delay that makes cross correlation a maximum, s
θ = angle between polar radii and horizontal, rad

Literature Cited

Amirshahidi, M. S., "Mechanics of Particle Motion in a Spouted Bed," PhD Thesis, Lehigh Univ. (1984).

Benkrid, A., "The Mechanics and Behavior of Spouted Beds," MS Thesis, Lehigh Univ. (1984).

Bridgwater, J., and K. B. Mathur, "Prediction of Spout Diameter in a Spouted Bed—A Theoretical Model," *Powder Technol.*, **6,** 183 (1972).

Brown, R. L., and J. C. Richards, *Principles of Powder Mechanics,* Pergamon Press (1970).

Carslaw, H. S., and J. C. Jaeger, *Conduction of Heat in Solids,* Clarendon Press, 2nd ed. (1959).

Epstein, N., and S. Levine, "Non-Darcy Flow and Pressure Distribution in a Spouted Bed," *Proc. Eng. Found. Conf. on Fluidization,* Cambridge Univ. Press, 98 (1978).

Grbavcic, Z. B., D. V. Vukovic, and F. K. Zdanski, "Fluid Flow Pattern, Minimum Spouting Velocity and Pressure Drop in Spouted Beds," *Can. J. Chem. Eng.*, **54,** 33 (1976).

Geldart, D., and K. J. Whiting, "A Comparison of Cylindrical and Semi-Cylindrical Spouted Beds of Coarse Particles," *Chem. Eng. Sci.*, **35,** 1499 (1980).

Geldart, D., A. Hemsworth, R. Sundavadra, and K. J. Whiting, "A Comparison of Spouting and Jetting in Round and Half-Round Fluidized Beds," *Can. J. Chem. Engr.*, **59,** 638 (1981).

Graham, D. P., A. R. Tait, and R. S. Wadmore, "Measurement and Prediction of Flow Patterns of Granular Solids in Cylindrical Vessels," *Powder Technol.*, **50,** 65 (1987).

Green, M. C., and J. Bridgwater, "An Experimental Study of Spouting in Large Sector Beds," *Can. J. Chem. Eng.*, **61,** 281 (1983).

Jenike, A. W., "Flow of Bulk Solids," Bulletin No. 64, Utah Engineering Experimental Station, Univ. of Utah (1954).

Jackson, R., "Some Features of the Flow of Granular Materials and Aerated Granular Materials," *J. of Rheol.*, **30**(5), 907 (1986).

Khoe, G. K., "Mechanics of Spouted Beds," PhD Thesis, Technische Hogeschool, Delft (1980).

Lefroy, B. E., and J. F. Davidson, "The Mechanics of Spouted Beds," *Trans. Inst. Chem. Eng.*, **17,** 120 (1969).

Lim, C. J., and K. B. Mathur, "Modelling of Particle Movement in Spouted Beds," *Proc. Eng. Found. Conf. on Fluidization,* Cambridge Univ. Press, 1st ed., 104 (1978).

Litwiniszyn, J., "Application of the Equation of Stochastic Processes to Mechanics of Loose Bodies," *Arch. Mech. Stos.*, **4,** 8 (1956).

Litwiniszyn, J., "The Model of a Random Walk of Particles Adapted to Researches on Problems of Mechanics of Loose Media," *Bull. Acad. Pol. Sci., Ser. Sci. Tech.*, **11**(10), 61 (1963)

Littman, H., and M. H. Morgan, "General Relationships for the Minimum Spouting Pressure Drop Ratio and the Spout-Annular Interfacial Condition in a Spouted Bed," *Proc. Eng. Found. Conf. on Fluidization,* Henniker, N. H., Plenum Press, New York, 287 (1980).

McNab, G. S., and J. Bridgwater, "A Theory for Effective Solid Stresses in the Annulus of Spouted Beds," *Can. J. Chem. Eng.*, **57,** 274 (1974).

Mamuro, T., and H. Hattori, "Flow Pattern of Fluid in Spouted Beds," *Chem. Eng. Japan,* **1,** 1 (1968).

Mathur, K. B., and N. Epstein, *Spouted Beds,* Academic Press, New York (1974).

Mullins, W. W., "Experimental Evidence for the Stochastic Theory of Particle Flow Under Gravity," *Powder Tech.*, **9,** 29 (1974).

Nedderman, R. M., and U. Tuzun, "A Kinematic Model for the Flow of Granular Material," *Powder Tech.*, **22,** 243 (1979).

Oki, K., P. Walawender, and L. T. Fan, "The Measurement of Local Velocity of Solid Particles," *Powder Tech.*, **18,** 171 (1977).

Patrose, B., and H. S. Caram, "Optical Fiber Probe Transit Anemometer for Particle Velocity Measurements in Fluidized Beds," *AIChE J.*, **28,** 604 (1982).

Rovero, G., N. Piccinini and A. Lupo, "Solids Velocities in Full and Half-Sectional Spouted Beds," *Entropie,* **124,** 43 (1985).

Spencer, A. J. M., "A Theory of the Kinematics of Ideal Soils Under Plane Strain Conditions," *Mech. Phys. Solids,* **12,** 337 (1964).

Suciu, G. C., and M. Patrascu, "Particle Circulation in a Spouted Bed," *Powder Tech.*, **19,** 109 (1978).

Sullivan, C., A. Benkrid, and H. S. Caram, "Prediction of Solids Circulation Patterns in a Spouted Bed," *Powder Tech.*, **53,** 257 (1987).

Thorley B., K. B. Mathur, J. Kalseen, and P. E. Gishler, "The Effect of Design Variables on Flow Characteristics in a Spouted Bed," Rep. Nat. Res. Council of Canada (1955).

Thorley, B., J. B. Saunby, K. B. Mathur, and G. L. Osburg, "An Analysis of Air and Solid Flow in a Spouted Wheat Bed," *Can. J. Chem. Eng.*, **37,** 184 (1959).

Van Velzen, D., H. F. Flamm, H. Langenkamp, and A. Casile, "Motion of Solids in Spouted Beds," *Can. J. Chem. Eng.*, **52,** 156 (1974).

Manuscript received June 20, 1988, and revision received Mar. 27 1989.